

Water Solvent and Local Anesthetics: A Computational Study

R. C. BERNARDI,¹ D. E. B. GOMES,² P. G. PASCUTTI,² A. S. ITO,³
C. A. TAFT,¹ A. T. OTA⁴

¹*Departamento de Física Aplicada, Centro Brasileiro de Pesquisas Físicas, CBPF,
Rio de Janeiro, Brazil*

²*Laboratório de Modelagem e Dinâmica Molecular, Instituto de Biofísica Carlos Chagas Filho,
Universidade Federal do Rio de Janeiro, Brazil*

³*Departamento de Física e Matemática, Faculdade de Filosofia, Ciências e Letras de Ribeirão Preto,
Universidade de São Paulo, Brazil*

⁴*Departamento de Física, Centro de Ciências Exatas, Universidade Estadual de Londrina, Brazil*

Received 1 November 2006; accepted 12 December 2006

Published online 2 February 2007 in Wiley InterScience (www.interscience.wiley.com).

DOI 10.1002/qua.21300

ABSTRACT: There are various experimental studies regarding the toxicity and the time of action of local anesthetics, which contain general insights about their pharmacological and physicochemical properties. Although a detailed microscopic analysis of the local anesthetics would contribute to understanding these properties, there are relatively few theoretical studies about these molecules. In this article, we present the results from calculations performed for three local anesthetics: tetracaine, procaine, and lidocaine, both in their charged and uncharged forms, in aqueous environment. We have used the density functional theory and molecular dynamics simulations to study the structural characteristics of these compounds. The radial distribution function $g(r)$ was used to examine the structure of water molecules surrounding different regions of the local anesthetics. We demonstrated the nonhomogeneous character of the anesthetics with respect to their affinity to water solvent molecules as well as the modifications in their affinity to water caused by changes in their charge state. We also observed that the biological potency of the anesthetics is more related to the behavior of specific groups within the molecule, which are responsible for the interaction with the lipid phase of membranes, rather than the general properties of the molecule as a whole. © 2007 Wiley Periodicals, Inc. *Int J Quantum Chem* 107: 1642–1649, 2007

Key words: density functional theory; molecular dynamics; radial distribution function; local anesthetics; hydrophobicity

Correspondence to: A. T. Ota; e-mail: tsutomu@uel.br

Contract grant sponsor: FAPESP.

Contract grant sponsor: CAPES.

Contract grant sponsor: CNPq.

Introduction

Local anesthetics (LA) in clinical use are tertiary amines and, despite their different structures, share chemical features that are relevant to their biological function: an aromatic ring, a polar group, and an ionizable amine with relatively high pK_a values of 7.5–9.0 [1]. Consequently, in a physiological medium local anesthetic cations partially dissociate into charged and uncharged forms, in a pH-dependent process. It has been shown that strongly hydrophobic charged anesthetics were easily partitioned into hydrophobic environments such as surface-adsorbed films and micelles, whereas weakly hydrophobic charged anesthetics were hardly or not partitioned into such environments [2, 3]. Since local anesthetic molecules must be transferred from solution to the hydrophobic environment of biological membranes to give rise to anesthetic action, it is suggested that the uncharged forms of LA, supposedly strongly hydrophobic, are necessary for the physiological activity.

LA are also known to induce their anesthetic effect by blocking inward sodium transport and therefore, the action potential of axons [1], and partitioning into the lipid bilayer can modulate the access of LA to their binding sites in Na^+ channels [4, 5]. These molecules are also known to bind to other membrane proteins, affecting their function [6], and to interact with membrane lipids, altering their organizational properties [7–10]. Such changes in biological membranes could interfere with lipid–protein interactions, leading to protein conformational changes that may reflect on their activity [11, 12].

Although studies conducted at physiological pH have indicated that local anesthetic activity is related to the protonated form, the importance of the uncharged species has been increasingly recognized in view of the presumed existence of a binding site for the uncharged local anesthetic deep inside the hydrophobic membrane core [4, 5] and a pronounced partitioning and perturbation of lipid bilayer organization for uncharged local anesthetic species [13]. A correlation is also recognized between local anesthetic hydrophobicity, potency, and toxicity [14, 15], and it is believed that the stronger binding of the uncharged species to the membrane would protect LA from blood clearance, justifying long lasting anesthesia [8].

There are two basic classes of LA: amino-amides and amino-esters. Tetracaine (TTC) is an ester de-

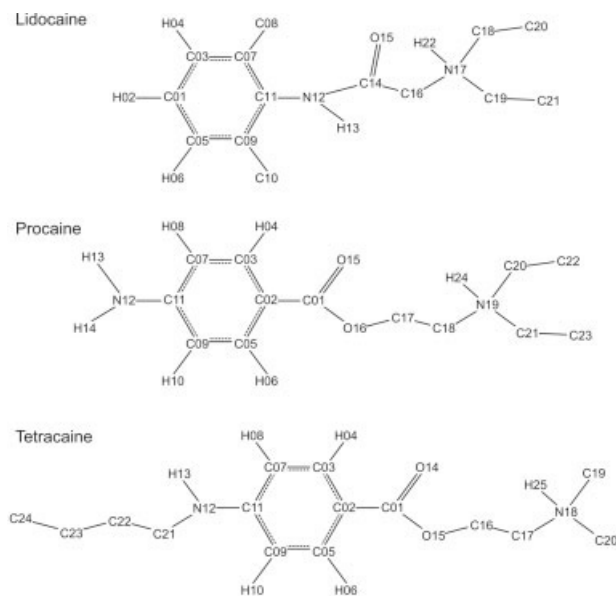


FIGURE 1. Schematic representation of the local anesthetics in charged form and with numerated atoms. The CHn are grouped over the carbon atoms.

rivative of *p*-aminobenzoic acid in which a butyl chain replaces one of the hydrogens on the *p*-amino group. Procaine (PRC) is the ester derivative of *p*-aminobenzoic acid and diethylaminoethanol. Lidocaine (LDC) is an aminoethylamide (Fig. 1). The physicochemical behavior of LA is a consistent and somewhat predictable function of their structures, whereas clinically, the potency is usually defined by the total mass (or moles) of drug required to relieve or prevent pain, produce tactile numbness, or effect inhibition of sympathetic or motor activity. By comparison, TTC is approximately 10 times more potent than PRC, while LDC has approximately twice the potency of PRC [16]. LA molecules with larger alkyl groups on both the tertiary amine nitrogen and the aromatic moiety show greater hydrophobicity and perturbing effects on the lipid bilayer order according to the order tetracaine (ester type) > lidocaine (amide type) > procaine (ester type), which is in agreement with the clinical potency of the LA [9].

Despite the accumulation of experimental studies about the molecular mechanisms for action of LA, not much work has been devoted to theoretical computation of those molecules. A recent report gave some insight regarding the structure of the LA tetracaine and its pharmacological action through calculations performed using the density functional theory (DFT) method [17]. The results indicated

that the molecule has regions with different degrees of hydrophobicity, and the pH dependent activity of TTC should be analyzed in view of local changes in different regions of the molecule rather than in terms of general effects on the hydrophobicity of the molecule as a whole.

In this work, we studied the structural characteristics of tetracaine, lidocaine, and procaine in protonated (charged) and deprotonated (uncharged) states using the DFT method. Ab initio calculations were made to obtain the geometry and charges of each atom to be used as starting points for molecular dynamics (MD) simulations. To evaluate the effects of water solvent on the properties of LA molecules, we examined the radial distribution function (RDF), known as $g(r)$ function, and the formation of hydrogen bonds which allowed us to identify regions of high and low water affinity. The results yield us elements to investigate the behavior of the LA molecules in an environment resembling the physiological medium, as well as a comparison with selected experimental results.

Materials and Methods

The geometries found in the literature were used as initial inputs for the structure calculations, and to obtain a low-energy ground state, we imposed planarity of the aromatic ring. The optimized molecular geometries for both protonated and deprotonated forms of the LA were obtained by the DFT/B3LYP method with the 6-31G** basis set [18–22]. The atomic charges were fitted to reproduce the molecular electrostatic potential through the ChelpG scheme [23, 24].

The MD studies were made using the GRO-MACS package [25]. The GROMOS 43a1 parameter set was used with modifications to charges, bond angles, and distances, according to the ab initio results. The molecules were solvated with SCP water model [26] in a cubic box and simulated in a NPT ensemble. The systems were thermodynamically coupled to a 300-K bath and pressure coupling was at 1 bar [27, 28]. Electrostatic and van der Waals interactions were considered to a “cut-off” of 1 nm, and the simulation time-step was set to 2 fs. An initial energy minimization was carried out followed by a 500-ps simulation to equilibrate all systems before a production run of 5 ns.

The relation between water solvent and LA was analyzed using the calculation from the RDF of the dynamics. The $g(r)$ function is defined as the aver-

age radial density of a certain observable to a distance r from an origin that provides an insight regarding the local structure of the surrounding media such as hydration shells for a solvated molecule. For r larger than the correlation distance, the RDF decays to the media density, usually normalized to one. A statistical approach of the $g(r)$ function can yield the potential of mean force (PMF), indicating the force between the atoms of interest. The PMF function is defined as: $W(r) = -kT \ln g(r)$, whereas the force can be obtained by the gradient of this function. If $g(r)$ is higher than one, $\ln g(r)$ is greater than zero and the potential is attractive. On the other hand, if $g(r)$ is lower than one, the potential is repulsive. The number of atoms contained in a shell is obtained by integrating the function $4\pi\rho r^2 g(r)$ in the appropriate distance interval [29].

However, in addition to the amplitude of $g(r)$, the distance r of the first hydration shell is also necessary to analyze the type of interactions between atoms or molecules. In polar groups for instance, a hydrogen bond occurs at the limit of $r = 0.35$ nm connecting donor and acceptor, with bond-angle tolerance of 30°. Considering these parameters, we made a time-dependent hydrogen bond calculation. The evaluation of the RDF and hydrogen bonds shows the possible allocation for the water coordination shell around each atom present in the LA, allowing us to analyze the hydrophobicity pattern on each part of this molecule, as well as of the LA as a whole.

Results and Discussion

ATOMIC CHARGES

The calculations performed with the ChelpG method demonstrated that atomic charges in all LA molecules did not change significantly with protonation. The only relevant modification was observed at the site of protonation (Table I); the charge of the nitrogen of the amine terminal (numbered N17 for LDC, N19 for PRC, and N18 for TTC in Fig. 1) changed from approximately $-0.5 e$ for the deprotonated LA to a slightly positive value in the protonated state. A small oscillation of charge values were also found on carbons that are first neighbors of protonated nitrogen. A similar result was already reported for TTC [17].

The solvation properties of the LA molecules were analyzed using the $g(r)$ function, which describes the average density of the solvent as a func-

TABLE I

Charge values for each atom from anesthetics, calculated via ChelpG on B3LYP/6-31G** quantum calculations.

Lidocaine			Procaine			Tetracaine		
Atom	Neutral	Charged	Atom	Neutral	Charged	Atom	Neutral	Charged
C01	-0.05369	-0.01633	C01	0.61308	0.62726	C01	0.70798	0.65843
H02	0.09310	0.10836	C02	-0.12325	-0.18465	C02	-0.20597	-0.20534
C03	-0.19779	-0.20442	C03	-0.03140	0.01172	C03	0.02076	0.01830
H04	0.11432	0.13431	H04	0.08729	0.10250	H04	0.08706	0.09935
C05	-0.24713	-0.22260	C05	-0.02817	-0.00240	C05	0.01118	-0.02105
H06	0.12660	0.13561	H06	0.08954	0.10098	H06	0.07277	0.08243
C07	0.09496	0.10246	C07	-0.26354	-0.32003	C07	-0.32759	-0.31150
C08	0.01305	0.03003	H08	0.13121	0.14862	H08	0.13001	0.14134
C09	0.11980	0.14153	C09	-0.27351	-0.31234	C09	-0.27783	-0.25057
C10	-0.00671	-0.00295	H10	0.13052	0.14785	H10	0.11608	0.11994
C11	0.08880	0.03614	C11	0.41852	0.60134	C11	0.46540	0.45804
N12	-0.52452	-0.44375	N12	-0.80944	-0.96888	N12	-0.6833	-0.62812
C13	0.27920	0.32197	H13	0.34805	0.43570	H13	0.32500	0.32542
C14	0.63810	0.61246	H14	0.34948	0.43487	O14	-0.53851	-0.52671
O15	-0.49268	-0.49500	O15	-0.48758	-0.54590	O15	-0.47951	-0.42920
C16	0.07473	-0.04148	O16	-0.43826	-0.38714	C16	0.30522	0.31663
N17	-0.55193	0.11573	C17	0.27982	0.31092	C17	0.20775	0.13781
C18	0.31021	0.21290	C18	0.19912	0.07557	N18	-0.46019	0.03401
C19	0.24307	0.33390	N19	-0.58265	0.01993	C19	0.12843	0.19885
C20	-0.07431	-0.00114	C20	0.26993	0.14408	C20	0.12843	0.20681
C21	-0.04718	0.02100	C21	0.25549	0.18299	C21	0.25615	0.25163
H22		0.12127	C22	-0.05620	0.04460	C22	-0.01882	0.00228
			C23	-0.07805	0.03387	C23	0.06705	0.05802
			H24		0.29854	C24	-0.03748	-0.01955
						H25		0.28275

The atoms numbers are the same as those in Figure 1.

tion of the distance r between a given atom, or a group of atoms of the molecule, and an atom from the solvent. Considering the solvent as water molecules, if the values of $g(r)$ are greater than 1.0, the region around the atoms under consideration is hydrophilic, otherwise it is hydrophobic. $g(r)$ greater than one implies that the local mean density at the distance r is higher than the volume density. Furthermore, if the distance of the first peak in $g(r)$ is greater than 0.5 nm, the region has hydrophobic characteristics. We selected atoms or groups in the LA molecules to perform the analysis, as follows.

To understand how the water environment polarizes the anesthetics [30], we made calculations on TTC, using the Onsager continuum solvation model. The values of the charges obtained for each atom are very close to the charges calculated with the simpler methods which neglect polarization effects. Some modifications were observed for aro-

matic ring carbon atoms; however, the difference with the ChelpG charges is small. The benzene ring is a more hydrophobic part of the TTC molecules and the variations in charge should not affect the $g(r)$ obtained without the polarization effects. As the later calculation is time consuming, it was not repeated for the other anesthetics.

PROTONATION SITE OF LA

Upon changes in the pH of the medium, a hydrogen ion can be associated to or dissociated from the nitrogen of the amine terminal. For the three LA in the protonated state, the plot of $g(r)$ functions suggests the occurrence of water shell coordination around that hydrogen atom (Fig. 2). The amino-ester type anesthetics PRC and TTC presented similar results, with the first peak in $g(r)$ near to 0.19 nm, suggesting the formation of hydrogen bond

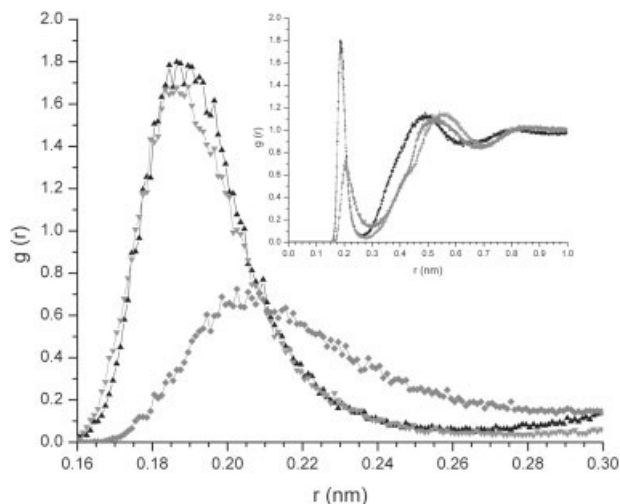


FIGURE 2. Plots of $g(r)$ for the hydrogen atom involved in the protonation of LA. The distance refers to oxygen atom. The inset shows $g(r)$ extended to the second and third solvation layers. ▲ represents TTC, ▼ represents PRC, and ◆ represents LDC.

between the H atom and water oxygen, indicating a very hydrophilic environment in that region. In TTC, the second and third peaks in $g(r)$ are slightly closer than that observed in the other anesthetics, (see Fig. 2), indicating that it has a more intense attractive interaction with water. For the amino-amide type anesthetic LDC, the first peak in $g(r)$ is less intense and located at a larger distance compared to the other anesthetics. In that molecule, the relatively short distance between nitrogen in the amine group (atom N17 in Fig. 1) and carbonyl oxygen (atom O15 in Fig. 1) decreases the charge of the hydrogen, reducing the attractive interaction with water molecules.

The first sharp peak in $g(r)$ of PRC and TTC also indicates the presence of an organized water structure, suggesting that some water molecules remain near the H atom. The analysis of the amino terminal groups, using a time-dependent hydrogen bond calculation, revealed a high prevalence of hydrogen bonds with water molecules for the charged forms of TTC (95.1%) and PRC (82.5%). For the uncharged molecules, the prevalence was much lower, TTC 25.8% and PRC 4.6%. The same hydrogen bonds analysis for LDC revealed a lower value than that observed for the amino-esters, 64.1% and 1.5% for the charged and uncharged forms, respectively. The hydrogen bond profile rationalizes the differences found in the RDF peaks and reinforces the relevance of the charge state to the penetration of LA on

the membrane since this portion on the charged forms is visibly hydrophilic.

CARBONYL OXYGEN

The $g(r)$ function for the carbonyl oxygen (numbered 14 in TTC and 15 in PRC and LDC, Fig. 1) is dependent on the state of protonation of the LA. In the deprotonated state of the amino-esters TTC and PRC, the carbonyl oxygen hydrophilic character is indicated by the intense peak in $g(r)$ located around 0.175 nm (Fig. 3). The same peak at 0.175 nm appears also in the $g(r)$ function of uncharged LDC; however, its intensity is significantly lower than the value observed for TTC and PRC (Fig. 3). Since LDC is an amino-amide, the participation of carbonyl oxygen in the bond involving the nitrogen amide of the aromatic ring (N12-C14-O15 in Fig. 1) seems to decrease its affinity to solvent water molecules.

The protonation of TTC and LDC changes the polarity around the carbonyl oxygen, enhancing the local hydrophilicity, as indicated by the increase in the intensity of the first peak of $g(r)$ function (Fig. 3). An opposite effect, however, was observed in PRC, whose $g(r)$ function presents a small decrease in the intensity of the first peak when the molecule is protonated. The reduction of the first peak in $g(r)$ for charged PRC (Fig. 3) reflects the small changes in the charge distribution on O15 (Table I) in the twisted structure of the molecule, which decreases the affinity to water, and the steric restrictions to the presence of additional solvent near to the water coordination shell already circumventing the neighboring H24 atom. The most significant

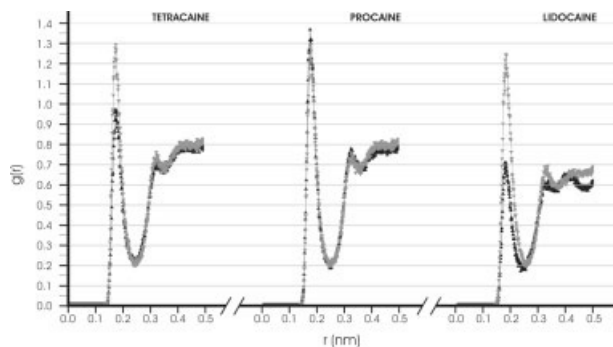


FIGURE 3. Plots of $g(r)$ of oxygen carbonyl atoms. The distance refers to hydrogen atom of water. ▲ represents charged molecules and ▼ represents uncharged molecules.

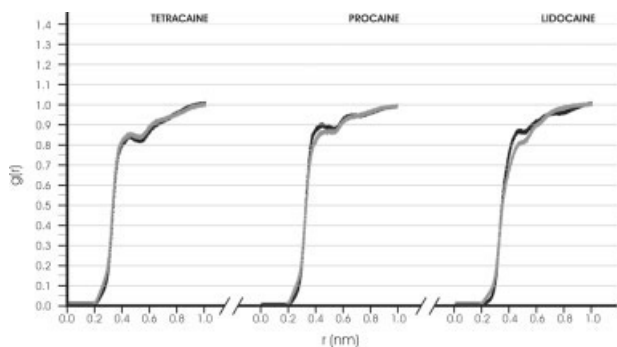


FIGURE 4. Plots of $g(r)$ for the region of the aromatic ring. The distance refers to the center of mass of water. ▲ represents charged molecules, while ▼ represents uncharged molecules.

changes of charge distribution affecting the carbonyl oxygen atom were found only on PRC (Table I).

AROMATIC RING AND AMINO TERMINAL

As expected, the plot of $g(r)$ function for the aromatic region of all LA is consistent with the hydrophobicity of the aromatic group. There are no discernible peaks, and the intensities are always below 1.0 even at large distances from the origin (Fig. 4). In the same figure one can see that the hydrophobicity of the aromatic region in TTC has low sensitivity to the protonation state of the molecule and a small decrease in the intensity of $g(r)$ was observed in PRC and LDC, which becomes more hydrophobic with bonding of a hydrogen atom to nitrogen amine.

In the region around the CH_3 groups of the amine terminal, the protonation state of LA can be an important factor influencing the arrangement of the water solvent molecules. In the deprotonated LA, the first peak in $g(r)$ is located at distances larger than 0.35 nm and the intensity is near to or below 1.0, indicating a hydrophobic environment (Fig. 5). Among the LA investigated, TTC is the least hydrophobic, which may be attributed to the greater proximity of CH_3 to the nitrogen atom of the amine group, whereas for tetracaine it is a dimethylamine and for PRC and LDC they are diethylamines. On the other hand, the protonation of nitrogen amine increases the hydrophilicity in the CH_3 terminal as observed by the raise in the intensity of the first peak in $g(r)$ to values above 1.0, sharpening of its shape, and slight decrease in the

distance from the origin (Fig. 5). Another indication of increase in hydrophilicity of CH_3 groups due to protonation of LA is the decrease in the distance of the second peak in $g(r)$, and the most prominent effect is observed for TTC. It is also noticeable that enhancement in hydrophilicity due to protonation is more evident in LDC than PRC.

The RDF of the amine terminal of LA is shown in Figure 6. The plots of $g(r)$ function indicate that the deprotonated amine group as a whole is hydrophobic. The highest hydrophobicity was observed for LDC, followed by PRC and TTC. In the charged molecules, $g(r)$ functions indicate a small contribution of a hydrophilic component at short distances, around 0.20 nm, although the hydrophobic component at larger distances above 0.40 nm predominates in the plots (Fig. 6).

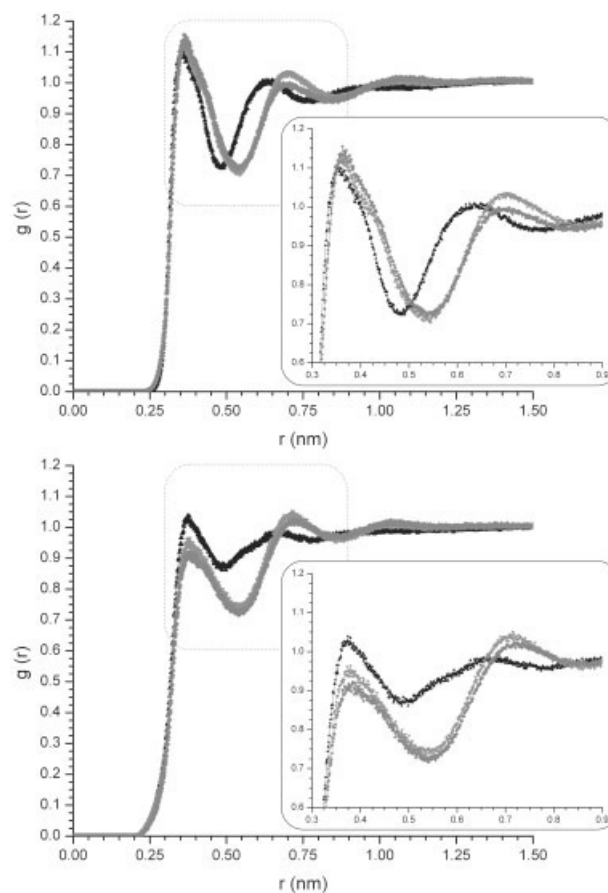


FIGURE 5. Plots of $g(r)$ for CH_3 amine terminal. The distance refers to the center of mass of water in tetracaine (▲), procaine (▼), and lidocaine (◆); top: the charged molecules; bottom: the uncharged anesthetics.

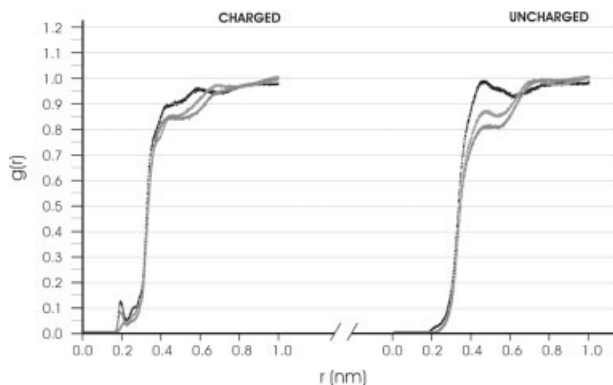


FIGURE 6. Plots of $g(r)$ for the entire amine terminal. The distance refers to the center of mass of water. ▲ represents TTC, ▼ represents PRC, and ◆ represents LDC.

Conclusions

The results discussed indicate the nonhomogeneous character of LA with respect to their affinity to water solvent molecules. It was possible to identify different regions of the molecule with degrees of hydrophobicity as well as the variations in the affinity to water caused by changes in their charge state effectively observed by de Paula et al. [6, 13]. This observation is relevant considering the interaction of LA with the lipids, which modulates the physiological activity [8]. The lipid bilayer is also inhomogeneous, with regions of different polarity, varying from the hydrophilic interface with the aqueous medium to the very hydrophobic inner region [8].

Tetracaine has an acyl chain bound to the p-amino group, conferring a high degree of hydrophobicity. A general observation was that, the more hydrophobic the uncharged anesthetics, the higher the physiological and hemolytic effects [9, 10], whereas TTC is the most active compound. In addition, the decrease in mobility of lipids at the interface, together with an increase in mobility in the hydrocarbon region, was promoted by anesthetics, the extent of effects following the order tetracaine > lidocaine > procaine.

However, when analyzing the different moieties of the anesthetics, we observed that, in uncharged form, the most hydrophobic compound in the regions of carbonyl oxygen, aromatic ring, and methyl groups is LDC, an amide type anesthetic, instead of the ester type anesthetics TTC and PRC. This result correlates with the detailed NMR obser-

vations that changes in the membrane organization are promoted in greater extent by LDC in comparison with TTC [8]. The verification that different regions of the lipid membrane bilayer respond differently to the binding of uncharged anesthetics [12] emphasizes the importance of the knowledge of the properties of different regions of the anesthetics.

In charged LDC and PRC, surprisingly, the hydrophobicity of the aromatic ring increases compared with that of the uncharged anesthetics, an effect which has its counterpart in the increase of hydrophilicity around the protonated nitrogen and, for LDC, in carbonyl oxygen as well. Hydrophilicity in carbonyl oxygen decreases in PRC because of conformational changes imposing steric restrictions to the presence of water near that atom. As already reported, minor changes in the aromatic ring occurs upon protonation of TTC. On the other hand, the methyl groups in the amino terminal become slightly less hydrophobic in protonated LA, a modification more evident in LDC. Thus, protonation of anesthetics enhances the amphiphilic character of the molecules, avoiding interpretations purely based on the attribution of hydrophobic character to uncharged and hydrophilic character to the charged molecules.

Several properties of membranes such as interface's charge density, hydration of the lipid bilayer, intermolecular hydrogen-bonded network among phospholipids molecules and/or protein molecules, rotational mobility of the hydrocarbon chain are altered because of the incorporation of LA into membranes. In addition to direct interaction with sodium channels, anesthetics may also interact with membrane lipids, affecting properties such as fluidity with effects on the transport of Na^+ and K^+ in nerve membranes, leading to anesthetic action. It thus becomes important to take into account local properties of the different parts of anesthetics such as those revealed by our calculations.

The potency of anesthetics is correlated to their strength and the time necessary for the effect to occur. However, for the deprotonated molecule, the hydrophilic character is reduced and in the more liposoluble form, the anesthetics' effect is weaker. As the aromatic region is very liposoluble for all the anesthetics, the region of amine terminal should be very important to understand the process of membrane penetration. We note in Figure 6 that the uncharged form of TTC is more hydrophilic, followed by PRC and LDC. This result is in agreement with the sequence for the potency of the anesthetics

and also with the decreasing sequence for their pKa, indicating that the anesthetics' character is related to intrinsic properties of specific groups inside the molecules. With higher pKa, more charged molecules will be anchored on the interface water-membrane at physiological pH. This may also lead, in many cases, to destabilization of the membrane, causing the reported hemolytic effects.

ACKNOWLEDGMENTS

The authors are grateful to Juliana A. Passipieri for helpful discussions on local anesthetics.

References

1. Butterworth, J. F.; Strichartz, G. R. *Anesthesiology* 1990, 72, 711.
2. Singer, M. A. *Biochem Pharmacol* 1977, 51.
3. Smith, I. C. P.; Auger, M.; Jarrell, H. C. *Ann NY Acad Sci* 1991, 625, 668.
4. Ragsdale, D. S.; McPhee, J. C.; Scheuer, T.; Catterall, W. A. *Science* 1994, 265, 1724.
5. Ragsdale, D. S.; McPhee, J. C.; Scheuer, T.; Catterall, W. A. *Proc Natl Acad Sci USA* 1996, 93, 9270.
6. de Paula, E.; Schreier, S. *Brazilian J Med Biol Res* 1996, 29, 877.
7. Shibata, A.; Ikawa, K.; Terada, H. *Biophys J* 1995, 69, 470.
8. Fraceto, L. F.; Pinto, L. D. A.; Franzoni, L.; Braga, A. A. C.; Spisni, A.; Schreier, S.; de Paula, E. *Biophys Chem* 2002, 99, 229.
9. Yun, I.; Cho, E. S.; Jang, H. O.; Kim, U. K.; Choi, C. H.; Chung, I. K.; Kim, I. S.; Wood, W. G. *Biochim Biophys Acta* 2002, 1564, 123.
10. Fraceto, L. F.; Spisni, A.; Schreier, S.; de Paula, E. *Biophys Chem* 2005, 115, 11.
11. Hille, B.; Courtney, K.; Dunn, R. *Molecular Mechanisms of Anesthesia*; Raven: New York, 1975.
12. Lee, A. G. *Nature* 1976, 262, 545.
13. de Paula, E.; Schreier, S. *Biochim Biophys Acta* 1995, 1240, 25.
14. Matsuki, H.; Simada, K.; Kaneshina, S.; Kamaya, H.; Ueda, I. *Colloid Surf B: Biointerfaces* 1998, 287.
15. Malheiros, S. V. P.; Pinto, L. M. A.; Gottardo, L.; Yokaichiya, D. K.; Fraceto, L. F.; Meirelles, N. C.; de Paula, E. *Biophys Chem* 2004, 110, 213.
16. Yagiela, J. A. *Pharmacology and Therapeutics for Dentistry*; Mosby: Philadelphia, 1986.
17. Bernardi, R. C.; Gomes, D. E. B.; Pascutti, P. G.; Ito, A. S.; Ota, A. T. *Int J Quantum Chem* 2006, 106, 1277.
18. (a) Hohenberg, P.; Kohn, W. *Phys Rev B* 1964, 136, 864; (b) Hohenberg, P.; Kohn, W. *Phys Rev A* 1965, 140, 1133.
19. Lee, C. T.; Yang, W. T.; Parr, R. G. *Phys Rev B* 1988, 37, 785.
20. Becke, A. D. *J Chem Phys* 1993, 98, 5648.
21. Becke, A. D. *Phys Rev A* 1988, 38, 3098.
22. Frisch, M. J.; Trucks, G. W.; Schlegel, H. B.; Scuseria, G. E.; Robb, M. A.; Cheeseman, J. R.; Montgomery, J. A., Jr.; Vreven, T.; Kudin, K. N.; Burant, J. C.; Millam, J. M.; Iyengar, S. S.; Tomasi, J.; Barone, V.; Mennucci, B.; Cossi, M.; Scalmani, G.; Rega, N.; Petersson, G. A.; Nakatsuji, H.; Hada, M.; Ehara, M.; Toyota, K.; Fukuda, R.; Hasegawa, J.; Ishida, M.; Nakajima, T.; Honda, Y.; Kitao, O.; Nakai, H.; Klene, M.; Li, X.; Knox, J. E.; Hratchian, H. P.; Cross, J. B.; Adamo, C.; Jaramillo, J.; Gomperts, R.; Stratmann, R. E.; Yazyev, O.; Austin, A. J.; Cammi, R.; Pomelli, C.; Ochterski, J. W.; Ayala, P. Y.; Morokuma, K.; Voth, G. A.; Salvador, P.; Dannenberg, J. J.; Zakrzewski, V. G.; Dapprich, S.; Daniels, A. D.; Strain, M. C.; Farkas, O.; Malick, D. K.; Rabuck, A. D.; Raghavachari, K.; Foresman, J. B.; Ortiz, J. V.; Cui, Q.; Baboul, A. G.; Clifford, S.; Ciolowski, J.; Stefanov, B. B.; Liu, G.; Liashenko, A.; Piskorz, P.; Komaromi, I.; Martin, R. L.; Fox, D. J.; Keith, T.; Al-Laham, M. A.; Peng, C. Y.; Nanayakkara, A.; Challacombe, M.; Gill, P. M. W.; Johnson, B.; Chen, W.; Wong, M. W.; Gonzalez, C.; Pople, J. A. *Gaussian 03, Revision B.04*; Gaussian: Pittsburg, PA, 2003.
23. Sigfridsson, E.; Ryde, U. *J Comput Chem* 1998, 337.
24. Breneman, C. M.; Wiberg, K. B. *J Comput Chem* 1990, 11, 361.
25. van der Spoel, D.; van Buuren, A. R.; Apol, E.; Meulenhoff, P. J.; Tieleman, D. P.; Sijbers, A. L. T. M.; Hess, B.; Feenstra, K. A.; Lindahl, E.; van Drunen, R.; Berendsen, H. J. C. *Gromacs User Manual*; Nijenborgh, Groningen, The Netherlands, 2002. (www.gromacs.org)
26. Berendsen, H. J. C.; Postma, I. P. M.; van Gunsteren, W. F.; Hermans, I. *Intermolecular Forces*; Reidel: Dordrecht, Holland, 1981.
27. Lindahl, E.; Hess, B.; van der Spoel, D. *J Mol Model* 2001, 7, 306.
28. van Drunen, R.; van der Spoel, D.; Berendsen, H. J. C. *Abstracts of Papers of the American Chemical Society* 1995, 209, 49-COMP.
29. Filippini, A. *J Phys: Condensed Matter* 1994, 41, 8415.
30. McDonald, N. A.; Carlson, H. A.; Jorgensen, W. L. *J Phys Org Chem* 1997, 10, 563.